TECHNICAL NOTES

NATIONAL ADVISORY COMMITTEE FOR AERONAUTICS

No. 758

MEASUREMENTS AND ANALYSIS OF THE MOTION OF A CANARD AIRPLANE MODEL IN GUSTS

By Philip Donely, Harold B. Pierce, and Philip W. Pepoon
Langley Memorial Aeronautical Laboratory

Washington
April 1940

NATIONAL ADVISORY COMMITTEE FOR AERONAUTICS

TECHNICAL NOTE NO. 758

MEASUREMENTS AND ANALYSIS OF THE MOTION OF A CANARD AIRPLANE MODEL IN GUSTS

By Philip Donely, Harold B. Pierce, and Philip W. Pepoon

SUMMARY

A model of a hypothetical canard airplane, which was designed to be of the same size and general aerodynamic characteristics as a Boeing B-247 airplane, was tested in the N.A.C.A. gust tunnel at one wing loading, one forward speed, one gust velocity, and three gust gradients. The purpose of these tests was to determine the reactions of the model and to compare them with the results of unpublished tests on an equivalent model of the Boeing B-247 airplane.

The loads on the stabilizer of the canard model and the subsequent pitching motion could not be neglected; the current method of analysis was therefore extended to include these factors. Calculations were made based on the unsteady-lift functions for finite and infinite aspect ratio and for two interpretations of wing area. The results were compared with experiment and the best agreement was found to result when the net wing area and the unsteady-lift functions for infinite aspect ratio were used.

A comparison of the results from the two tests revealed that the resultant acceleration increment for the canard model was much higher than that for the Boeing B-247 model. The analysis indicated, however, that the stabilizer loads on the canard model accounted for the difference so that the aerodynamic loads on the wings of the two models were approximately equal. Thus, although the acceleration increment and the stabilizer load on the canard model are higher than those on the corresponding conventional arrangement, the net wing load on the canard model appears to be smaller by virtue of the greater inertia load acting to oppose the aerodynamic load.

INTRODUCTION

The wing loading and the power of present-day airplanes are constantly increasing. As a result, the slipstream produces uncertainty in the stability and the control characteristics and, in general, has adverse effects on them. With a view toward overcoming these difficulties, designers are reconsidering the possibilities of the canard airplane. Because data on the gust-load factors on this type of airplane are lacking, tests were conducted in the N.A.C.A. gust tunnel to determine the reactions of a canard model of the same size and general aerodynamic characteristics as a previously tested dynamically scaled model of a Boeing B-247 airplane.

The current method of analysis for gust-load factors (reference 1) was developed for the conventional monoplane. A simplifying assumption of reference 1, that the pitching motion be neglected, implies that there is zero tail load and zero pitch and that the conventional monoplane may be represented as a flying wing during passage through a gust. The downwash from the wing on the tail surfaces effectively reduces the change of angle of attack of the stabilizing plane by about 50 percent and, in addition, the tail enters the gust later than the wing so that the development of lift on the tail starts after that on the wing. Inasmuch as the wing has probably passed its peak load-factor increment before the tail lift can become appreciable, the simplifying assumption is reasonable. Experiments (reference 2) bear out the correctness of this analysis.

There is, however, reason to believe that, with the horizontal stabilizing plane ahead of the wing surface, a canard airplane will not satisfy the conditions previously set forth. The stabilizing plane is no longer subject to the downwash from the wing and, in addition, it enters the gust ahead of the wing so that the development of lift on the stabilizer precedes that on the wing. The combination of these two factors apparently makes it possible for the stabilizing plane to have developed an appreciable lift when the airplane experiences peak acceleration. An adverse pitching motion may arise to increase further the acceleration increment. It is therefore felt that these factors should be taken into account when the reactions of a canard airplane are being determined.

In this paper, the experimental results of the gust-tunnel tests of the model are compared with computed results based on the theory of unsteady lift as applied to the conventional monoplane. Additional computed results are presented that are based on several analyses in which the unsteady-lift functions are applied to both the wing and the stabilizing plane of the canard airplane. Unpublished results of a previous test of a model of the Boeing B-247 airplane are also compared with the results of the present investigation.

APPARATUS

The gust tunnel and its related equipment are described in reference 2.

The canard airplane model is shown in figures 1 and 2. Its pertinent characteristics as well as those for the hypothetical full-size airplane are given in figure 2 and table I. The weights and the mass distribution about the pitching axes were scaled to represent conditions at an altitude of 7,200 feet. The gross wing area referred to in table I is the plan-view area of the wing including the fuselage intercept, and the net wing area is the gross wing area minus the fuselage intercept. Engine nacelles and other protuberances were left off the model.

The wing was made as rigid as practicable in order to eliminate effects due to its deflection in the steepest gust gradient. The natural period of the wing is given in table I and the deflection curve for a load factor of 1.54 is given in figure 3.

The three gust-velocity distributions or profiles for which the tests were made (gradient distance $H = 0.7$, 3.7, and 8.2 ft) were approximately linear and are shown in figure 4 as plots of the ratio of local gust velocity U to the average maximum gust velocity $U_{max_{av}}$ against the distance, in feet, from the leading edge of the gust tunnel.

TESTS

The tests consisted of flights of the model over the gust tunnel at fixed values of the forward velocity and of the average maximum gust velocity. A minimum of five flights was made for each of the three gust gradients. Measurements were made of flight velocity, gust velocity, normal acceleration, vertical displacement, and pitch.

PRECISION

The measured quantities are estimated to be accurate within the following limits for any single test or run.

Acceleration increment. ±0.1g

Forward velocity. . . . ±1.0 foot per second

Gust velocity . . . . . ±0.1 foot per second

Pitch . . . . . ±0.2°

Vertical displacement . ±0.01 foot

Approximate computations of the effect of wing flexibility indicated an error of about 1.5 percent in the acceleration increment for the sharp-edge gust (H = 0.7 ft) and smaller errors in those for the gradient gusts. The error due to wing flexibility is thus within the limits of accuracy of the rest of the data and will be neglected.

In addition to errors in measurement, there exist errors due to the disturbed motion of the airplane model prior to entry into the gust. These motions may persist during the traverse of the gust. Inasmuch as it is impracticable to catapult an airplane model into a condition of steady gliding flight at the attitude, the speed, and the flight-path angle for which it is trimmed, oscillations in pitch, forward speed, and acceleration will take place when the airplane model leaves the catapult. These oscillations can be separated into a short-period oscillation that is highly damped and a long-period oscillation, the well-known phugoid, that is only slightly damped.

The short-period oscillation consists primarily of vertical and rotational motions of the airplane and, for the canard airplane model, these oscillations will have a period of about 0.6 second and a time to damp to one-twentieth of the original amplitude of about 0.24 second, which corresponds to about 14 feet of travel by the airplane model after take-off. Since the disturbances arise from the action of the catapult at the point of take-off, which is a minimum of 14 feet from the gust tunnel, a disturbance that impressed an acceleration of 1g on the airplane would cause an error during the traverse of the gust tunnel of less than 0.05g in the measured acceleration increment. Inspection of acceleration records from various airplane models that have undisturbed paths of the order of 30 feet (that is, zero gust velocity) indicates that the oscillations have disappeared before the airplane model reaches the gust tunnel and that the maximum error in acceleration increment would be less than 0.05g.

Inspection of the records previously mentioned indicates, however, that appreciable variations may exist in the "reference" direction of the airplane axis (that is, in the direction prior to entry into the gust), from which the pitch-angle increment is measured. These variations may lead to a possible error of the order of 0.3° in the maximum pitch increment for the longest gust-gradient distance. This error will not affect the shape of the curves but will result in a vertical displacement of the curves above or below the true curves.

The oscillations in pitch, forward speed, and acceleration that correspond to the phugoid oscillation will have a period of the order of 6 seconds. Computations of the errors caused by this oscillation indicate a maximum possible consistent error of 0.15g in the acceleration increment for a gust with a gradient distance of 8 feet and an error of 0.07g for a gradient distance of 4 feet. Inspection of the records used in the previous discussion of the short-period oscillation fails to indicate an error of this magnitude and it is felt that the maximum error due to this source under the test conditions is of the order of 0.05g. The error in pitch increment due to the phugoid oscillation is twofold: an error of the order of 0.02° that will modify the shape of the pitch-increment curves, and an error with a possible maximum value of 1° that will tend to rotate the pitch-increment curves about the point of reference.

In view of the results of this analysis, it appears that the errors (in the acceleration increments) arising from extraneous oscillations of the model are negligible except for the longest gradient distance (H = 8 ft). It also appears that use of the pitch-increment curves in the longer gradient distances for detailed comparisons with computations is unwarranted in view of the errors that are possible in determining the initial pitching condition of the model.

SYMBOLS

L lift.

g acceleration of gravity.

W airplane weight.

$\frac{dC_L}{d\alpha}$ slope of lift curve.

ρ mass density of air.

U gust velocity.

V forward velocity.

S area.

c chord length.

s distance penetrated into gust, chord lengths.

C_{L_g} unsteady-lift function for an airfoil penetrating a sharp-edge gust.

C_{L_α} unsteady-lift function for a sudden change of angle of attack.

For the purpose of this paper, C_{L_g} and C_{L_α} are the ratios of the lift coefficient at any distance s to the lift coefficient after an infinite distance has been traversed (steady flow).

q dynamic pressure.

θ pitch angle, degrees.

$\frac{d\theta}{dt}$ pitching velocity, radians per second.

l_w horizontal distance from center of gravity to aerodynamic center of wing.

l_s horizontal distance from center of gravity to aerodynamic center of stabilizer.

M pitching moment.

mk_Y^2 moment of inertia.

α angular acceleration.

Δn acceleration increment on airplane.

Δn_m acceleration increment on airplane due to vertical motion.

Δn_o acceleration increment on airplane due to action of gust.

Δn_{total} total acceleration increment on airplane.

Δn_{o_w} load-factor increment on wing due to action of gust.

Δn_{m_w} load-factor increment on wing due to vertical motion of airplane.

Δn_{θ_w} load-factor increment on wing due to pitch-angle increment of airplane.

Δn_{q_w} load-factor increment on wing due to pitching velocity of airplane.

$\Delta n_{w_{total}}$ total load-factor increment on wing.

Corresponding definitions for the stabilizer hold for symbols having subscript s instead of w.

Subscripts:

w wing.

s stabilizer.

s_2 distance of surface into gust at which lift is desired.

s_3 distance of center of gravity into gust at which acceleration increment occurs.

s_4 distance of center of gravity into gust at which acceleration increment reaches a maximum.

When subscripts w and s are used with distance penetrated into the gust s, the resulting term represents chord lengths of the surface referred to by the subscript.

RESULTS

Records of two flights for each gust gradient were evaluated to give sample histories of events during passage through the gust. These results are shown in the uncorrected form in figures 5, 6, and 7 plotted against the distance, in wing chord lengths, penetrated into the gust. The chord length used in this case is the mean geometric chord based on the gross wing area. The oscillations superimposed on the acceleration-increment curve for the sharp-edge gust (fig. 5) were due to the flexing of the wings as a result of the gust.

In view of the precision of the measurements and the tests, it is felt that too much weight should not be placed on the experimental pitch-angle increment curves for the 8.2-foot gradient condition (fig. 7).

In order to eliminate the effects of slight departures from the nominal values of air speed and gust velocity, the maximum acceleration increments were corrected to a forward velocity of 60 feet per second (40.9 mph) and a gust velocity of 6.5 feet per second. These results are shown in figure 8 plotted against the gradient distance in feet. For purposes of comparison, computed results based on the current method of analysis of reference 1 are included in figure 8. A considerable discrepancy will be noted between the experimental and the computed results.

ANALYSIS

The discrepancy between the experimental and the computed results based on the current method of analysis (reference 1), shown in figure 8, indicates that all factors have not been taken into account. As previously mentioned, there is reason to believe that the tail loads and the pitching motion should be included when the reactions of a canard airplane are being determined. An attempt was therefore made to include these factors in expressions of a general nature that could be applied to all types of canard airplanes. The individual integrals in the following equation have been derived to represent the forces due to the motion of the airplane during passage through the gust. The first two integrals express the load-factor increments on the wing and the stabilizer due to the action of the gust. The third and the fourth integrals represent the alleviation due to the vertical motion of the airplane. The last four integrals represent the load-factor increments due to the pitching motion of the airplane. The general expressions follow:

$$\Delta L_{total} = \Delta n_{total} W = \frac{dC_L}{d\alpha_w} \frac{\rho V S_w}{2} \int_0^{s_{w_2}} C_{L_g} (s_{w_2} - s_w) \frac{dU}{ds_w} ds_w$$

$$+ \frac{dC_L}{d\alpha_s} \frac{\rho V S_s}{2} \int_0^{s_{s_2}} C_{L_g} (s_{s_2} - s_s) \frac{dU}{ds_s} ds_s$$

$$+ \frac{dC_L}{d\alpha_w} \frac{\rho S_w c_w}{2} \int_0^{s_{w_3}} C_{L_\alpha} (s_{w_3} - s_w) \Delta n \, (s_w) ds_w$$

$$+ \frac{dC_L}{d\alpha_s} \frac{\rho S_s c_s}{2} \int_0^{s_{s_3}} C_{L_\alpha} (s_{s_3} - s_s) \Delta n \, (s_s) ds_s$$

$$+ \frac{dC_L}{d\alpha_w} \frac{S_w q}{57.3} \int_0^{s_{w_4}} C_{L_\alpha} (s_{w_4} - s_w) \frac{d\theta}{ds_w} ds_w$$

$$+\frac{dC_L}{d\alpha_s}\frac{S_s q}{57.3}\int_0^{s_{s_4}} C_{L_\alpha}(s_{s_4}-s_s)\frac{d\theta}{ds_s}ds_s$$

$$+\frac{dC_L}{d\alpha_w}\frac{S_w q l_w}{V}\left[-\int_0^{s_{w_4}} C_{L_\alpha}(s_{w_4}-s_w)\frac{d\left(\frac{d\epsilon}{dt}\right)}{ds_w}ds_w\right]$$

$$+\frac{dC_L}{d\alpha_s}\frac{S_s q l_s}{V}\left[-\int_0^{s_{s_4}} C_{L_\alpha}(s_{s_4}-s_s)\frac{d\left(\frac{d\theta}{dt}\right)}{ds_s}ds_s\right] \qquad (1)$$

$$M_{total} = \Sigma\,\Delta n_w W l_w + \Sigma\,\Delta n_s W l_s = m k_Y^2 \alpha \qquad (2)$$

A rigid simultaneous solution of equations (1) and (2) is obviously extremely difficult because the various integrals of the equations are mutually interdependent and some of them contain discontinuous functions.

In order to solve these equations for the canard airplane, the principle of superposition was employed by first assuming the airplane to pass over the gust with only one motion, namely, uniform forward velocity. The effect of the gust alone could then be calculated and used when determining the effects of the vertical motion and the pitch of the airplane. In order that these subsequent calculations might be performed, certain of the initial restrictions on the motion of the airplane were removed. These restrictions are:

(1) No vertical-displacement increment of the airplane occurs as it passes over the gust.

(2) No pitching motion of the airplane occurs as it passes over the gust.

When these restrictions are imposed, the only integrals to be solved are the ones that describe the acceleration increment or the load factor due to the action of

the gust on the wing and the stabilizer. These integrals are:

$$\frac{dC_L}{d\alpha_w}\frac{\rho V S_w}{2}\int_0^{s_{w_2}} C_{L_g}(s_{w_2} - s_w)\frac{dU}{ds_w}ds_w$$

and

$$\frac{dC_L}{d\alpha_s}\frac{\rho V S_s}{2}\int_0^{s_{s_2}} C_{L_g}(s_{s_2} - s_s)\frac{dU}{ds_s}ds_s$$

These integrals may be solved analytically or by means of Carson's theorem, as used in reference 3, depending upon the complexity of the variables dU/ds and C_{L_g}. In the solution for the canard airplane, the integrals were solved analytically by assuming a linear gust and by using expressions for C_{L_g} that were amenable to integration. The acceleration increment on the airplane was found by plotting the loading increments on the wing and the stabilizer as they passed through the gust and then combining them algebraically. An illustration of this method is shown in figure 9.

The next step in the solution was to remove the first restriction on the motion of the airplane. The integrals based on the vertical motion of the airplane, which are the third and the fourth terms in equation (1), could then be evaluated. They are:

$$\frac{dC_L}{d\alpha_w}\frac{\rho S_w c_w}{2}\int_0^{s_{w_3}} C_{L_\alpha}(s_{w_3} - s_w)\Delta n(s_w)ds_w$$

and

$$\frac{dC_L}{d\alpha_s}\frac{\rho S_s c_s}{2}\int_0^{s_{s_3}} C_{L_\alpha}(s_{s_3} - s_s)\Delta n(s_s)ds_s$$

The terms $\Delta n(s_w)$ and $\Delta n(s_s)$ express the variation of the final acceleration increment value as a func-

tion of the chord-length penetration of the surfaces into the gust. For the solution of these integrals, the functions $\Delta n(s_w)$ and $\Delta n(s_s)$ were assumed to be linear. The integrals were then put in the form

$$\Delta n \frac{\rho S_w c_w}{2 s_{w_3}} \frac{dC_L}{d\alpha_w} \int_0^{s_{w_3}} C_{L_\alpha}(s_{w_3} - s_w) s_w ds_w$$

$$+ \Delta n \frac{\rho S_s c_s}{2 s_{s_3}} \frac{dC_L}{d\alpha_s} \int_0^{s_{s_3}} C_{L_\alpha}(s_{s_3} - s_s) s_s ds_s$$

and, by the use of suitable expressions for C_{L_α}, they were readily solved.

The solution could then be put in the form

$$\Delta n_m = K \Delta n \tag{3}$$

for a particular value of s_3; and K, a constant for a particular value of s_3, could be plotted as a function of s_3 for a series of values of s_3.

The impressed acceleration can be determined from the following relation:

$$\Delta n = \Delta n_0 - K \Delta n \tag{4}$$

for a particular value of s_3.

In the present analysis, it was found that the process of evaluation might be further simplified by putting equation (4) in the form

$$\Delta n = \frac{\Delta n_0}{1 + K} \tag{5}$$

for a particular value of s_3. Note that the value of acceleration increment found here is similar to the value that would be obtained from the equation derived by Küssner (reference 4) and solved in reference 1, with the

exception that the stabilizer loads are here taken into account.

It should also be noted that, because of the stabilizer loads and the position of the center of gravity, the maximum acceleration increment on the airplane no longer occurs when the center of gravity of the airplane is at the point where the assumed gust shape first attains uniform velocity.

The second restriction on the motion of the airplane was removed in order to investigate the influence of pitching motion on the acceleration increment.

As a first approximation, the damping of pitch due to the pitching motion of the airplane was neglected and the direct effect of the loads on the stabilizer and the wing that arise from the action of the gust and the vertical motion of the airplane was investigated.

The method used was to compute the moments about the center of gravity of the airplane that arise from the loads imposed by the action of the gust and by the vertical motion of the airplane. These moments were combined and plotted against the distance penetrated by the model into the gust for the 3.7- and the 8.2-foot gust gradients. The sharp-edge-gust condition was omitted since the effect of pitch was felt to be inappreciable until after the airplane had reached its peak acceleration. The first integral of the moment curve gives a measure of the pitching velocity, and the second integral gives a measure of the pitch angle of the airplane.

The pitching-velocity and the pitch-angle curves were then used in conjunction with a previously selected expression of the unsteady-lift function C_{L_α} for the solution of the last four integrals of equation (1):

$$\frac{dC_L}{d\alpha_w}\frac{S_w q}{57.3}\int_0^{s_{w_4}} C_{L_\alpha}(s_{w_4} - s_w)\frac{d\theta}{ds_w}ds_w$$

$$\frac{dC_L}{d\alpha_s}\frac{S_s q}{57.3}\int_0^{s_{s_4}} C_{L_\alpha}(s_{s_4} - s_s)\frac{d\theta}{ds_s}ds_s$$

$$\frac{dC_L}{d\alpha_w}\frac{S_w q l_w}{V}\left[-\int_0^{s_{w_4}} C_{L_\alpha}\,(s_{w_4}-s_w)\frac{d\left(\frac{d\theta}{dt}\right)}{ds_w}ds_w\right]$$

$$\frac{dC_L}{d\alpha_s}\frac{S_s q l_s}{V}\left[-\int_0^{s_{s_4}} C_{L_\alpha}\,(s_{s_4}-s_s)\frac{d\left(\frac{d\theta}{dt}\right)}{ds_s}ds_s\right]$$

The term $d\theta/ds$ is the variation of pitch angle with the distance penetrated into the gust; the term $d\left(\frac{d\theta}{dt}\right)/ds$ is the variation of pitching velocity with the distance penetrated into the gust. These integrals were then solved by use of Carson's theorem for the acceleration increments at the previously determined peak acceleration, and the values were combined with those obtained from equation (5) to give the final acceleration increment on the airplane.

Throughout this analysis, no mention has been made of the specific expressions used for the quantities C_{L_g} and C_{L_α}. As in previous papers, such as reference 5, the analysis was carried out by using the unsteady-lift functions for infinite aspect ratio as derived by Küssner (reference 4) and Wagner (reference 6) and comparing the results with those obtained by using the unsteady-lift functions for finite aspect ratio as derived by Jones (reference 7). Curves for aspect ratio 6, based on reference 7, are included in this paper as figure 10.

The effect of unsteady lift on a fuselage-wing combination has not been determined; computations were therefore made using both the gross wing area and the net wing area with corresponding wing chords as suggested in reference 2.

DISCUSSION

The equations were first evaluated based on the gross wing area and the unsteady-lift functions for infinite aspect ratio because the use of these functions in previous papers indicated the best agreement with the experi-

mental data for conventional airplanes. It was found for the canard airplane that, although the agreement was good in the sharp-edge gust condition, the effect of pitch in the longer gradients (H = 3.7 and 8.2 ft) modified the loads to such an extent that the agreement with the test results was poor (table II, columns 1 and 6).

A similar analysis was made using Jones' unsteady-lift functions for a finite wing (reference 7). The alleviation due to pitch was so great in the 3.7-foot gust-gradient condition, however, that computations for the 8.2-foot gust-gradient condition were felt to be useless (table II, column 2).

A third analysis was then made using the unsteady-lift functions for infinite aspect ratio and the net wing area. The results from this analysis agreed with the test data within 0.2g for all the gust-gradient conditions (table II, columns 3 and 6). It is interesting to note that the load-factor increments caused by pitch angle reversed in sign for the 3.7-foot gust-gradient condition. The interpretation of the wing area and the chord is therefore obviously very important in calculating the load factors and the stability for a canard airplane.

As previously mentioned, the analysis pointed out that the maximum acceleration increment need not occur at the point where the gust velocity first becomes uniform. Reference to figure 6 shows that the experimental results bear out the analysis in this respect.

In an effort to arrive at better agreement, calculations were made using the net wing area and Jones' unsteady-lift functions for finite aspect ratio. Although the total acceleration increments for the conditions of the sharp-edge gust and the 3.7-foot gust gradient were in good agreement with the test results, the magnitude of the pitch terms in the condition of the 8.2-foot gust gradient was such as to give very poor agreement (table II, columns 4 and 6).

As stated before, the damping of pitch due to pitching motion had been neglected. An attempt was made, however, to calculate this effect for the gust with a gradient distance of 8.2 feet mentioned in the last paragraph. The approximate method of superposition was found to become as tedious as a strict solution, but there were indications that the load-factor increments would increase by a small amount.

From the consistency of the agreement of the derived with the experimental results, the analysis using the net wing area and the unsteady-lift functions for infinite aspect ratio was chosen as being the best present solution for the load-factor increments of this particular canard airplane. Although a detailed comparison of the pitch-angle increment curves is not warranted because of the limitations imposed by the precision and the test procedure, the calculated curves and the more reliable experimental curves (neglecting the 8.2-foot gradient condition) do show the same trends and order of magnitude of pitch-angle increments in this case.

The approximate analysis for this canard airplane is felt to be sufficiently accurate. Future tests on different types and arrangements of airplanes may, however, bring out a need for an analysis to cover other factors that would not be amenable to the procedure followed in this paper.

Figure 11 shows a comparison of the results of unpublished tests on an equivalent model of the Boeing B-247 airplane with analytical results based on reference 1. A comparison of these experimental results with those for the canard model (fig. 8) shows that, in all cases, the acceleration increment on the Boeing model has a lower value. This result apparently indicates that the gust-load factors on the canard airplane might have to be increased.

When the calculated results for each model are considered, it should be remembered that the current method of analysis (reference 1) used for the Boeing model gives directly the load factor on the wing but that the analysis developed in this paper for the canard model gives a total acceleration increment, which is the sum of both the stabilizer and the wing loads. A comparison of the values in column 3 of table II and in figure 11 shows that the aerodynamic loads on the wings of the two models are approximately the same but, when the resultant acceleration increments and the inertia loads for each model are combined, the indications are that the wing loads for the canard model will be less than those for the Boeing model.

The arrangement of surfaces of a canard airplane being such that there is no downwash effect from the wing on the stabilizer, it is felt that the design of this type of airplane, particularly in the nonacrobatic category,

should include an investigation of the gust-load factor on the horizontal stabilizer. The procedure used in this paper is not recommended because a gust of small size would probably load the stabilizer to a greater extent than a gust that would affect the airplane as a whole.

CONCLUDING REMARKS

The conclusions drawn on the basis of the foregoing results and discussion are:

1. The analysis chosen shows that, although the resultant acceleration increments and the stabilizer loads are greater for the canard airplane, the net wing stresses will be reduced below those of an equivalent Boeing B-247 airplane.

2. The gust loads on the stabilizer of a canard airplane may be of importance.

3. The pitching motion should not be neglected when the gust-load factors on a canard airplane are calculated.

4. For the present case, theory and experiment indicate that the maximum acceleration increment need not occur at the point where the gust first attains uniform velocity.

At the present time, there can be no recommended procedure for the evaluation of the effect of pitching motion. For all cases, additional study and experiment are required on the following problems:

1. The determination of the effective chord lengths and surface areas for use in problems of unsteady flow.

2. The determination of the effect of a gust on the stability of an airplane.

3. The determination of the effect of pitching motion when an airplane enters a gust.

4. The determination of the critical gust loads on the stabilizer of a canard airplane.

Langley Memorial Aeronautical Laboratory,
National Advisory Committee for Aeronautics,
Langley Field, Va., March 14, 1940.

REFERENCES

1. Rhode, Richard V.: Gust Loads on Airplanes. S.A.E. Jour., vol. 40, no. 3, March 1937, pp. 81-88.

2. Donely, Philip: An Experimental Investigation of the Normal Acceleration of an Airplane Model in a Gust. T.N. No. 706, N.A.C.A., 1939.

3. Jones, Robert T.: Calculation of the Motion of an Airplane under the Influence of Irregular Disturbances. Jour. Aero. Sci., vol. 3, no. 12, Oct. 1936, pp. 419-425.

4. Küssner, Hans Georg: Stresses Produced in Airplane Wings by Gusts. T.M. No. 654, N.A.C.A., 1932.

5. Donely, Philip, and Shufflebarger, C. C.: Tests in the Gust Tunnel of a Model on the XBM-1 Airplane. T.N. No. 731, N.A.C.A., 1939.

6. Wagner, Herbert: Über die Entstehung des dynamischen Auftriebes von Tragflügeln. Z.f.a.M.M., Bd. 5, Heft 1, Feb. 1925, S. 17-35.

7. Jones, Robert T.: The Unsteady Lift of a Wing of Finite Aspect Ratio. T.R. No. 681, N.A.C.A., 1940.

Table I

Characteristics of the Canard Model

	Model	Hypothetical airplane
Weight, lb	1.301	13,650
Gross wing area, sq ft	1.445	836
Mean geometric chord based on the gross wing area, ft	0.470	11.3
Net wing area, sq ft	1.302	-
Mean geometric chord based on net wing area, ft	0.422	-
Slope of wing lift curve, per radian	4.5	4.47
Natural wing period, sec	0.017	-
Stabilizer area, sq ft	0.257	148.5
Mean geometric stabilizer chord, ft	0.242	5.8
Slope of stabilizer lift curve, per radian	4.0	4.0
Moment of inertia, mk_Y^2, slug-ft^2	0.00790	247,000
Gust velocity, fps	6.5	31.9
Forward velocity, mph	40.9	200

Table II

Values of Load-Factor Increments (in g units) from Summary of Analysis of Canard Model

Type of load-factor increment	1	2	3	4	5	6
	Gross wing area (S_w = 1.445 sq ft, c_w = 0.470 ft)		Net wing area (S_w = 1.302 sq ft, c_w = 0.422 ft)		Current method of analysis*	Experimental
	Using unsteady-lift functions for					
	A = ∞	A = 6	A = ∞	A = 6	A = ∞	
For Sharp-Edge Gust						
Δn_{o_w}	1.90	2.16	1.85	1.92	-	-
Δn_{m_w}	-.21	-.29	-.24	-.20	-	-
Δn_{θ_w}	-	-	-	-	-	-
Δn_{q_w}	-	-	-	-	-	-
$\Delta n_{w_{total}}$	1.69	1.87	1.61	1.72	1.58	-
Δn_{o_s}	0.35	0.37	0.35	0.37	-	-
Δn_{m_s}	-.04	-.05	-.05	-.04	-	-
Δn_{θ_s}	-	-	-	-	-	-
Δn_{q_s}	-	-	-	-	-	-
$\Delta n_{s_{total}}$	0.31	0.32	0.30	0.33	-	-
Δn_{total}	2.00	2.19	1.91	2.05	1.58	2.03
For 3.7-Foot Gradient Gust						
Δn_{o_w}	2.00	2.07	1.88	1.87	-	-
Δn_{m_w}	-.62	-.57	-.55	-.51	-	-
Δn_{θ_w}	-.03	-.20	.25	.23	-	-
Δn_{q_w}	-.07	-.11	-.03	-.02	-	-
$\Delta n_{w_{total}}$	1.28	1.19	1.55	1.57	1.47	-
Δn_{o_s}	0.35	0.36	0.35	0.36	-	-
Δn_{m_s}	-.11	-.09	-.10	-.09	-	-
Δn_{θ_s}	-.01	-.04	.04	.04	-	-
Δn_{q_s}	.03	.06	.02	.01	-	-
$\Delta n_{s_{total}}$	0.26	0.29	0.31	0.32	-	-
Δn_{total}	1.54	1.48	1.86	1.89	1.47	2.11
For 8.2-Foot Gradient Gust						
Δn_{o_w}	1.70	1.85	1.58	1.65	-	-
Δn_{m_w}	-.69	-.73	-.61	-.67	-	-
Δn_{θ_w}	-.21	-	-.04	-.42	-	-
Δn_{q_w}	-.06	-	-.04	-.09	-	-
$\Delta n_{w_{total}}$	0.74	-	0.89	0.47	1.32	-
Δn_{o_s}	0.34	0.35	0.33	0.31	-	-
Δn_{m_s}	-.12	-.12	-.11	-.12	-	-
Δn_{θ_s}	-.04	-	-.01	-.08	-	-
Δn_{q_s}	.03	-	.02	.05	-	-
$\Delta n_{s_{total}}$	0.21	-	0.23	0.16	-	-
Δn_{total}	0.95	-	1.12	0.63	1.32	1.35

*Reference 1.

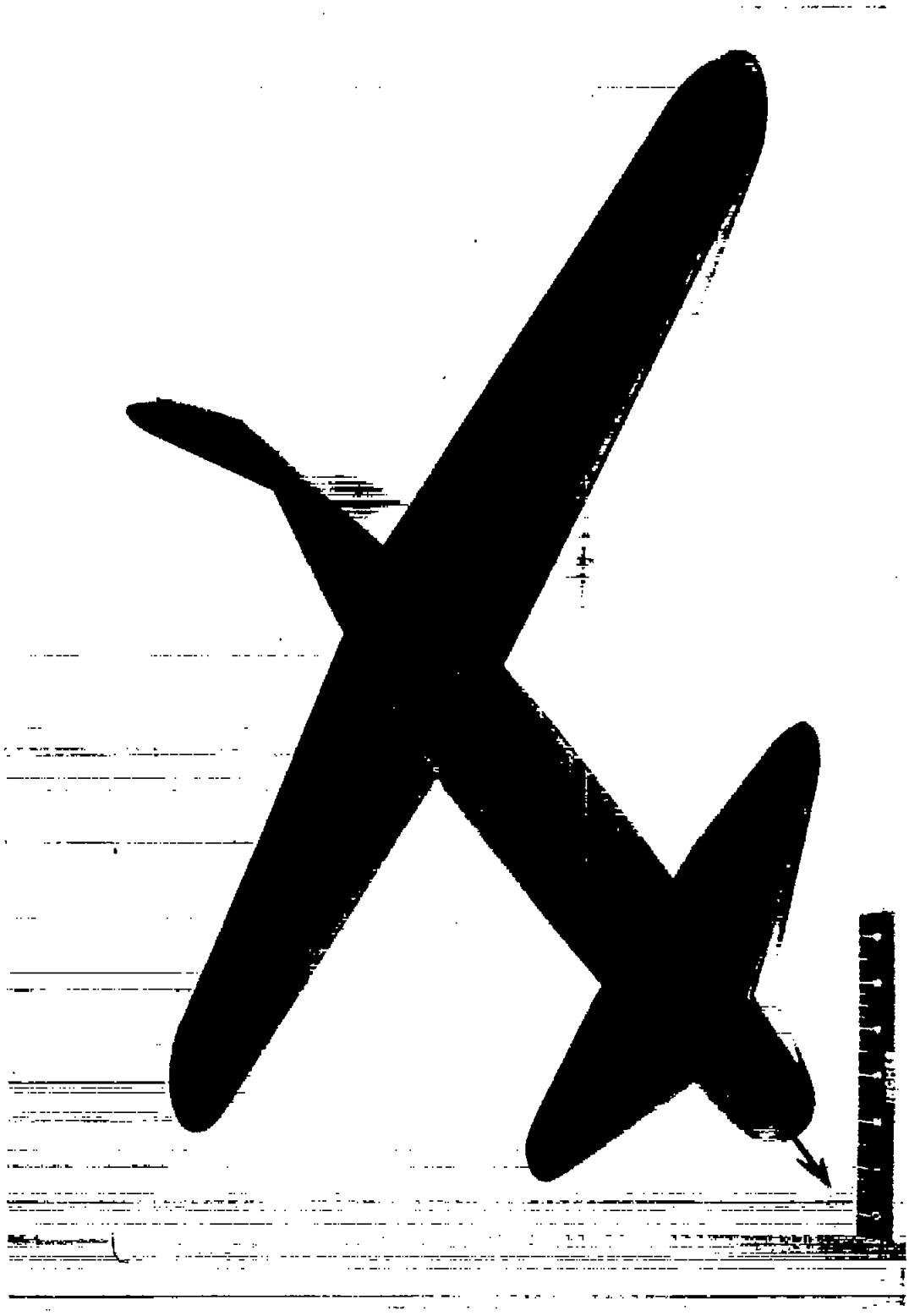

Figure 1.- Canard airplane model.

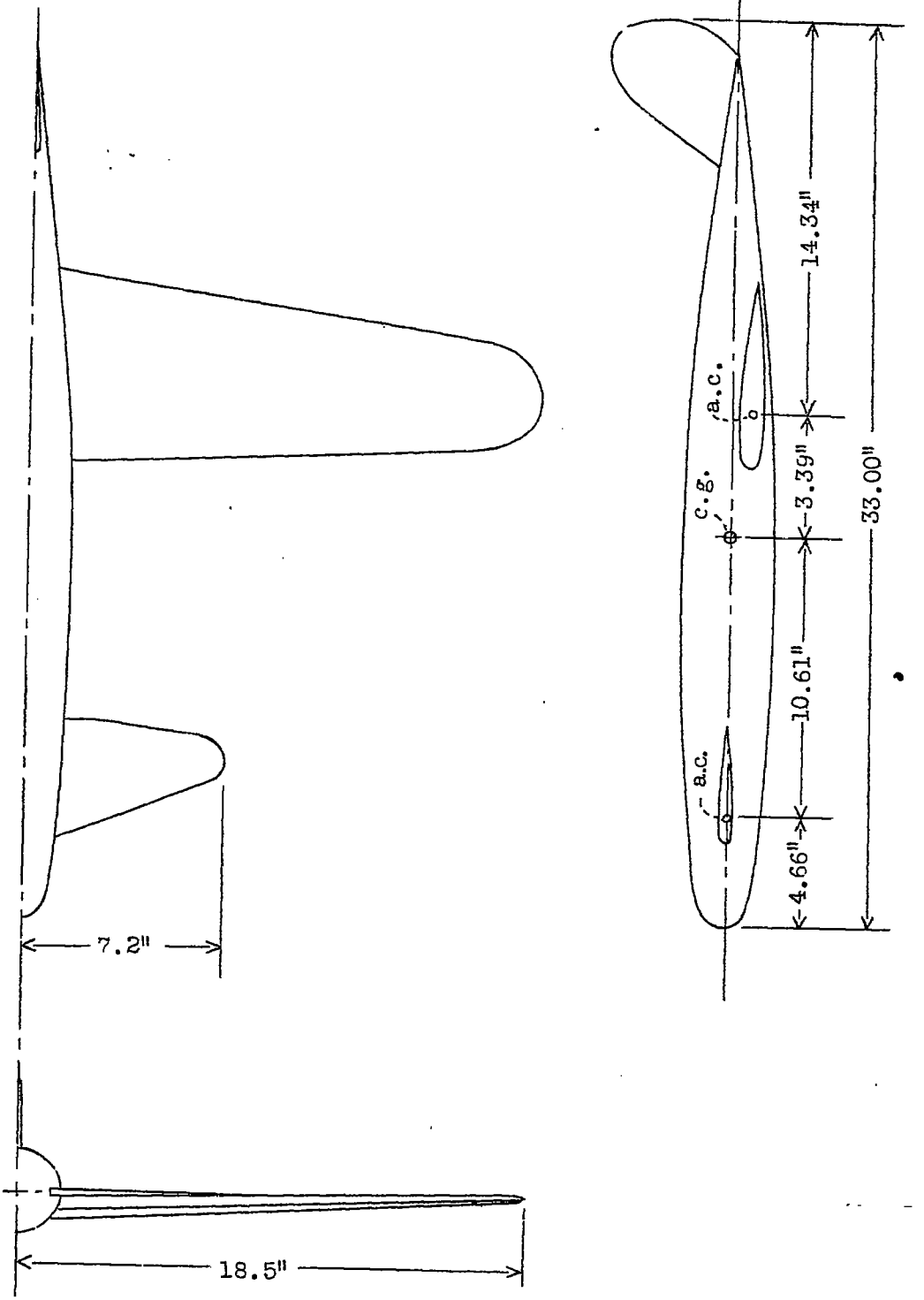

Figure 2.- Line drawing of canard airplane model.

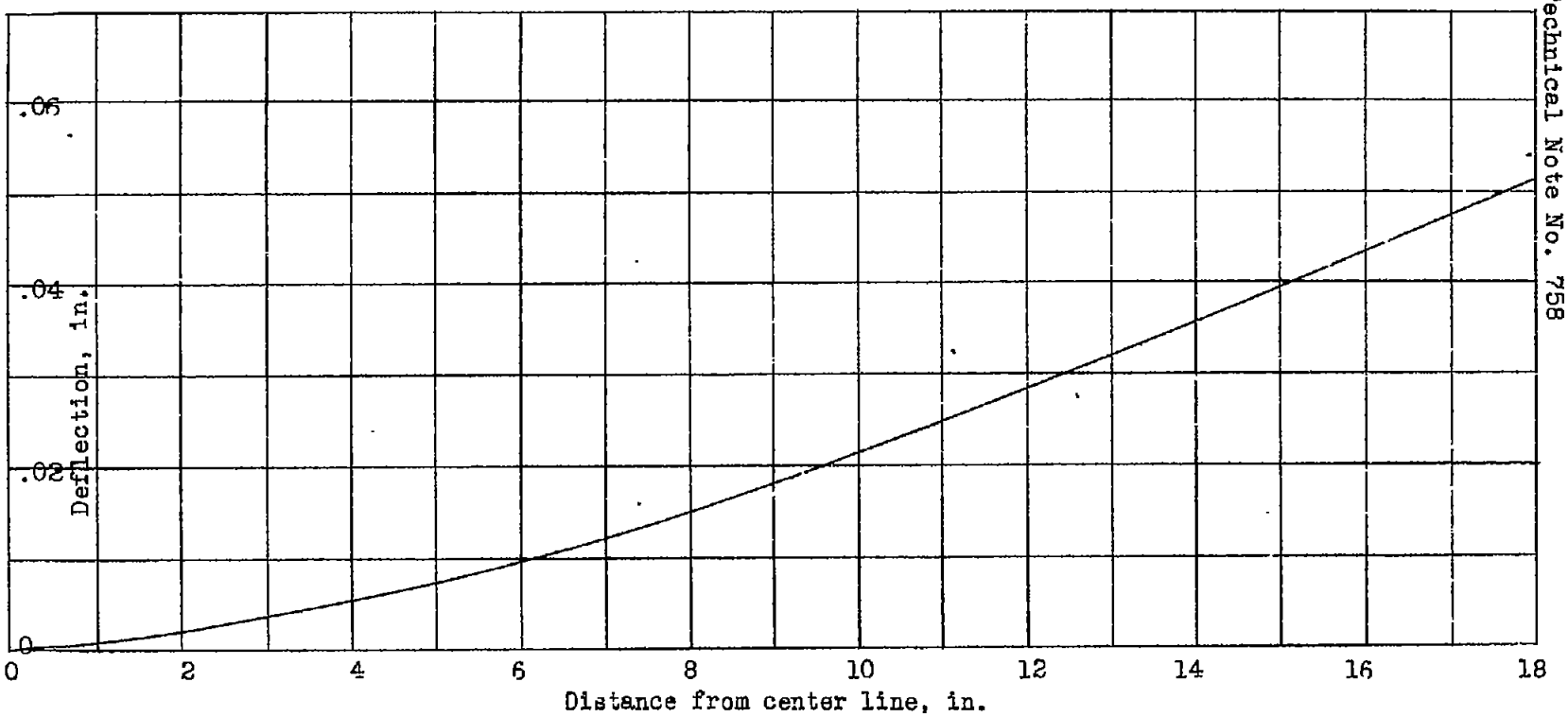

Figure 3.- Wing-deflection curve. Load factor, 1.54

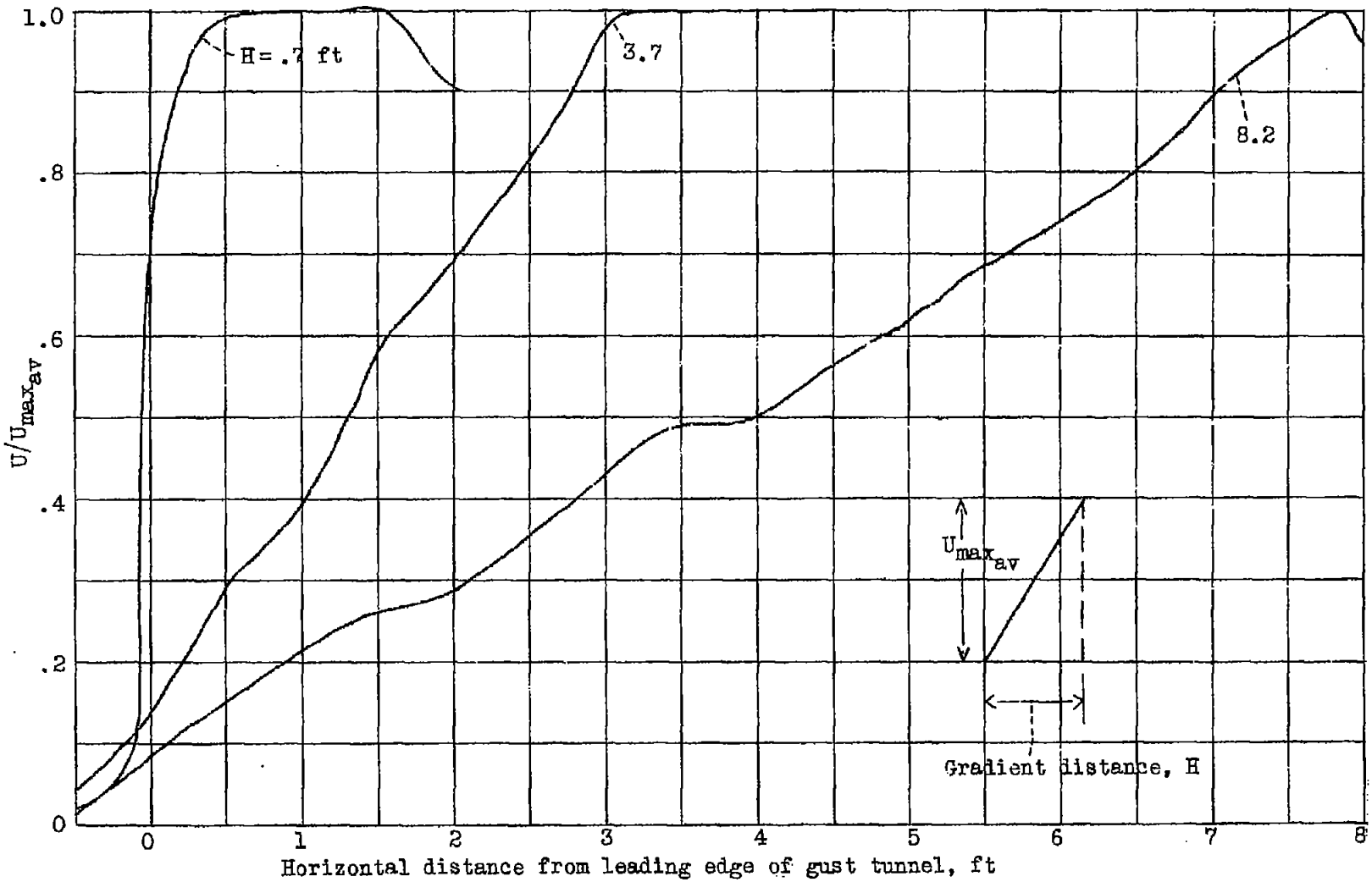

Figure 4.- Velocity distribution through jet.

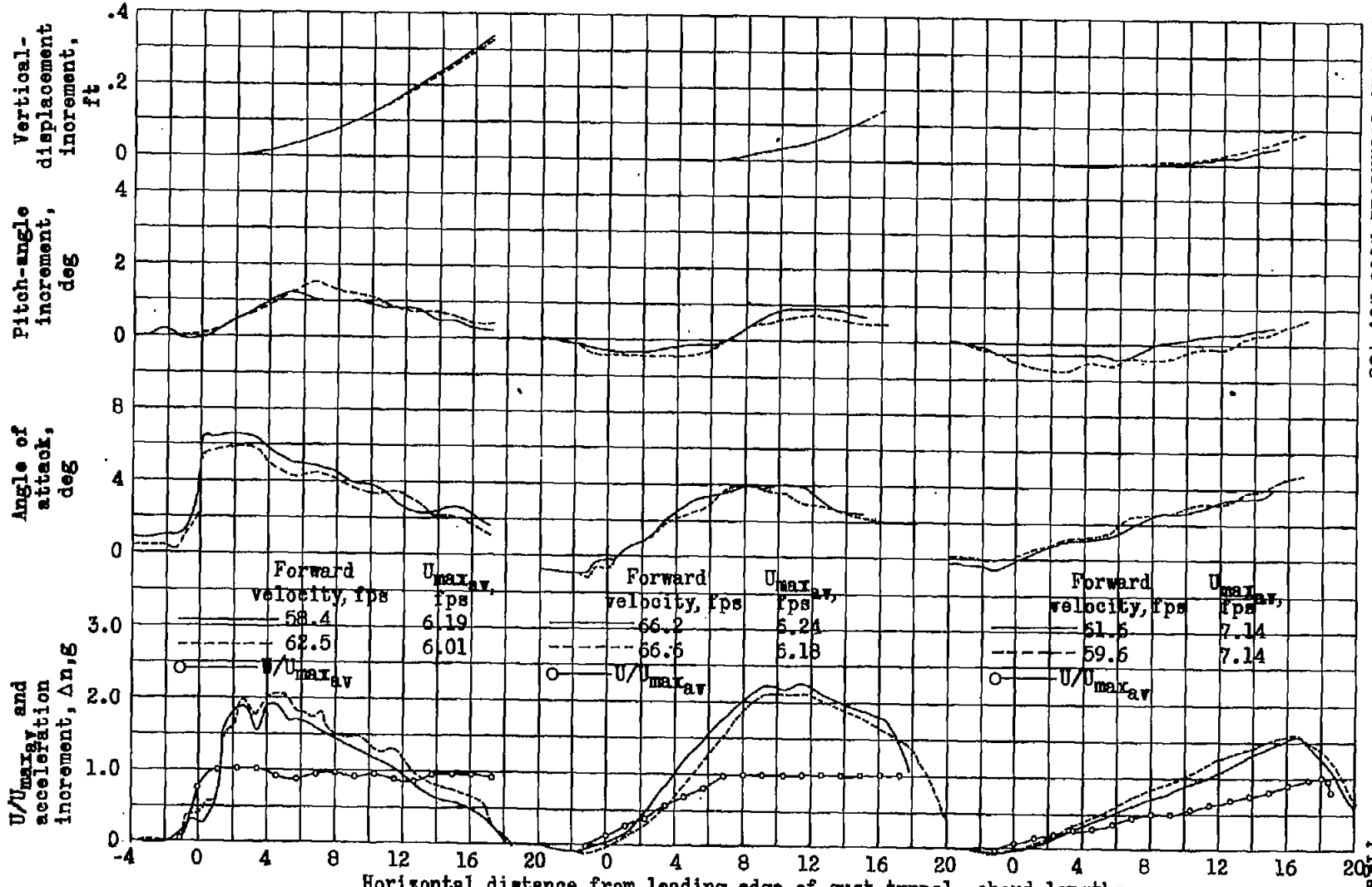

Figure 5.- History of events in the 0.7-foot sharp-edge gust.

Figure 6.- History of events in the 3.7-foot gust gradient.

Figure 7.- History of events in the 8.2-foot gust gradient.

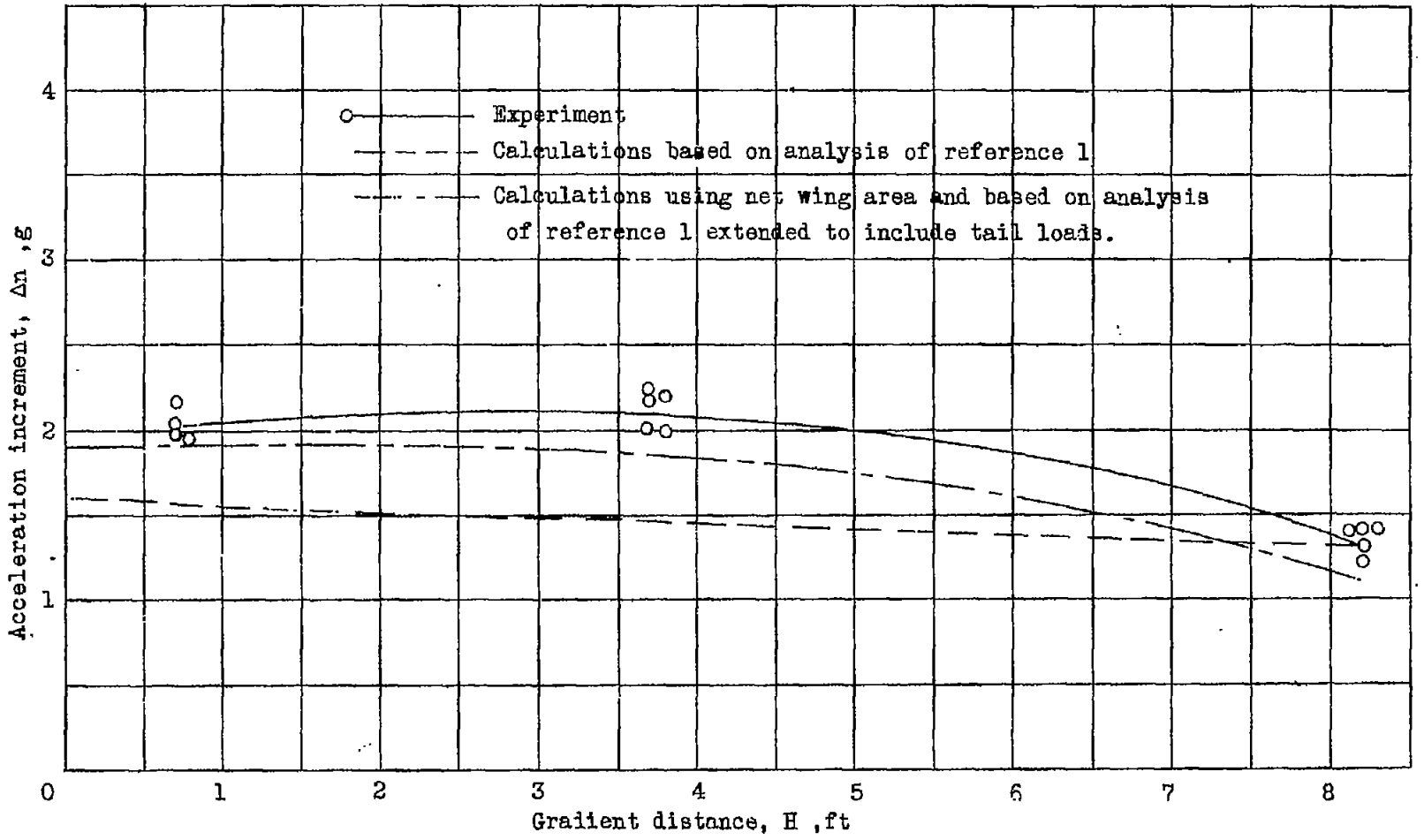

Figure 8.- Comparison of experiment and analysis. Canard airplane model.

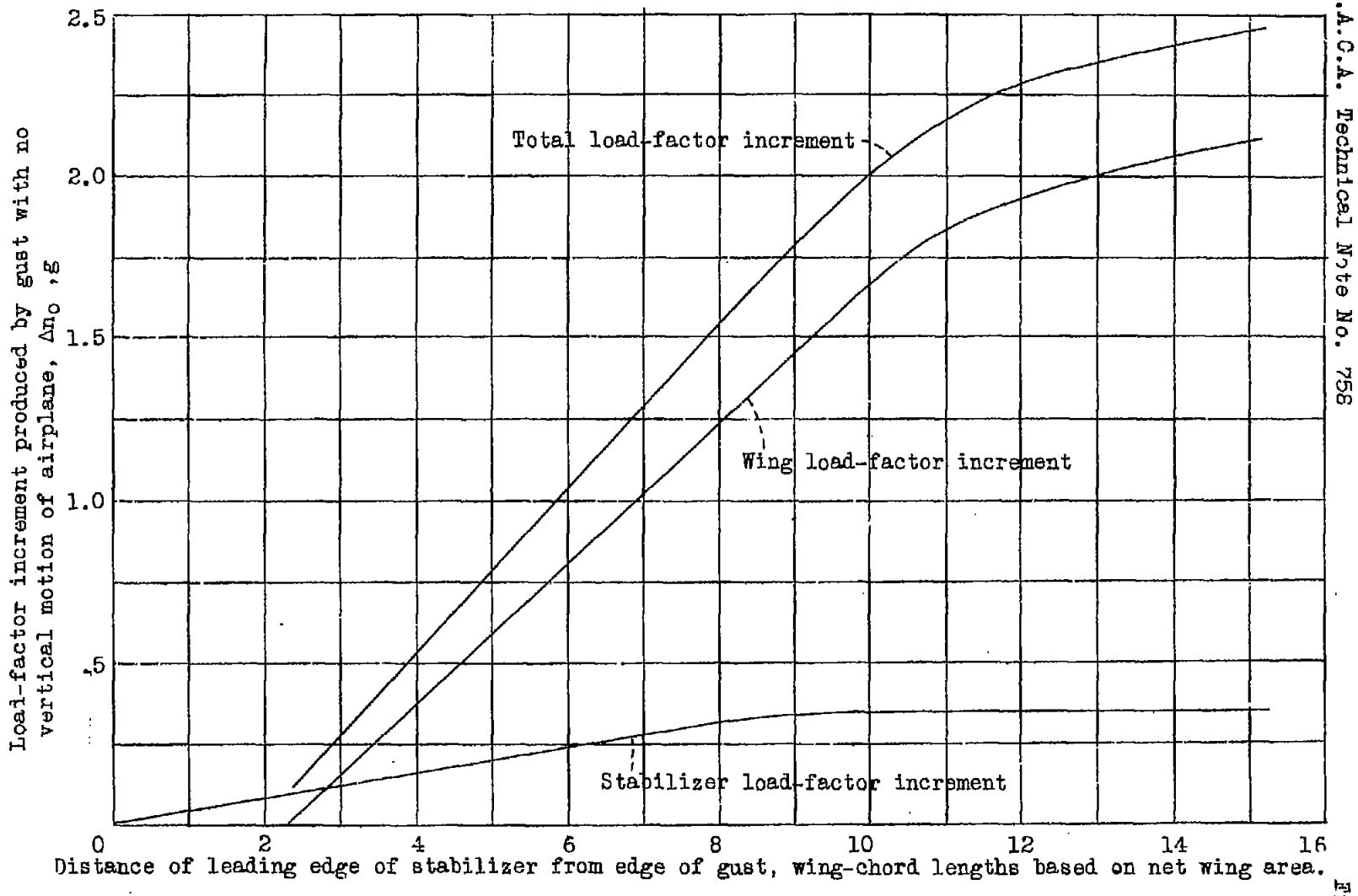

Figure 9.- Variation of Δn_o with distance traveled into gust. 3.7 ft gust-gradient condition, V=60 fps, U = 6.5 fps

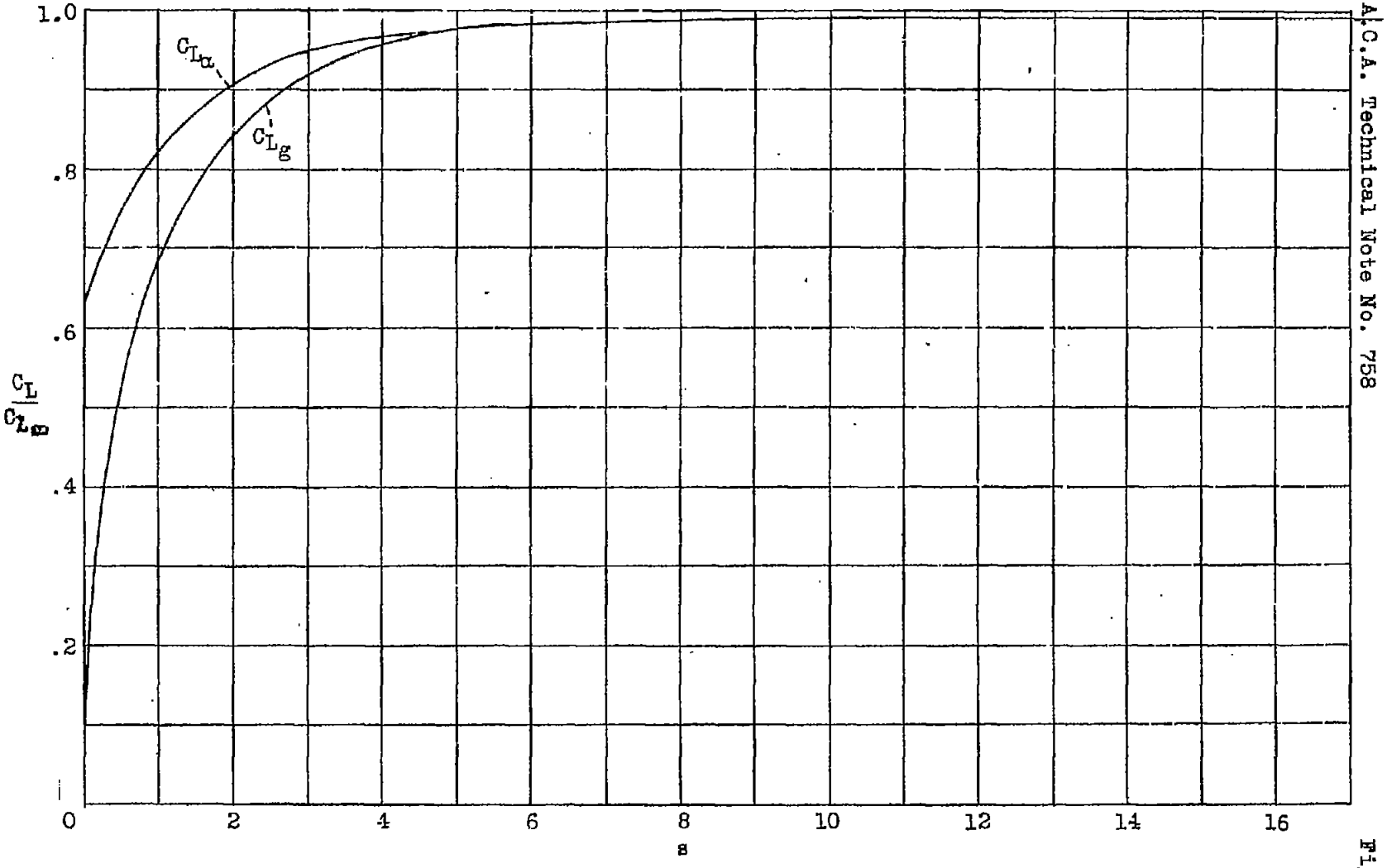

Figure 10.- Curves of C_{L_α} and C_{L_g} for aspect ratio 6 based on Jones' unsteady-lift functions (reference 7).

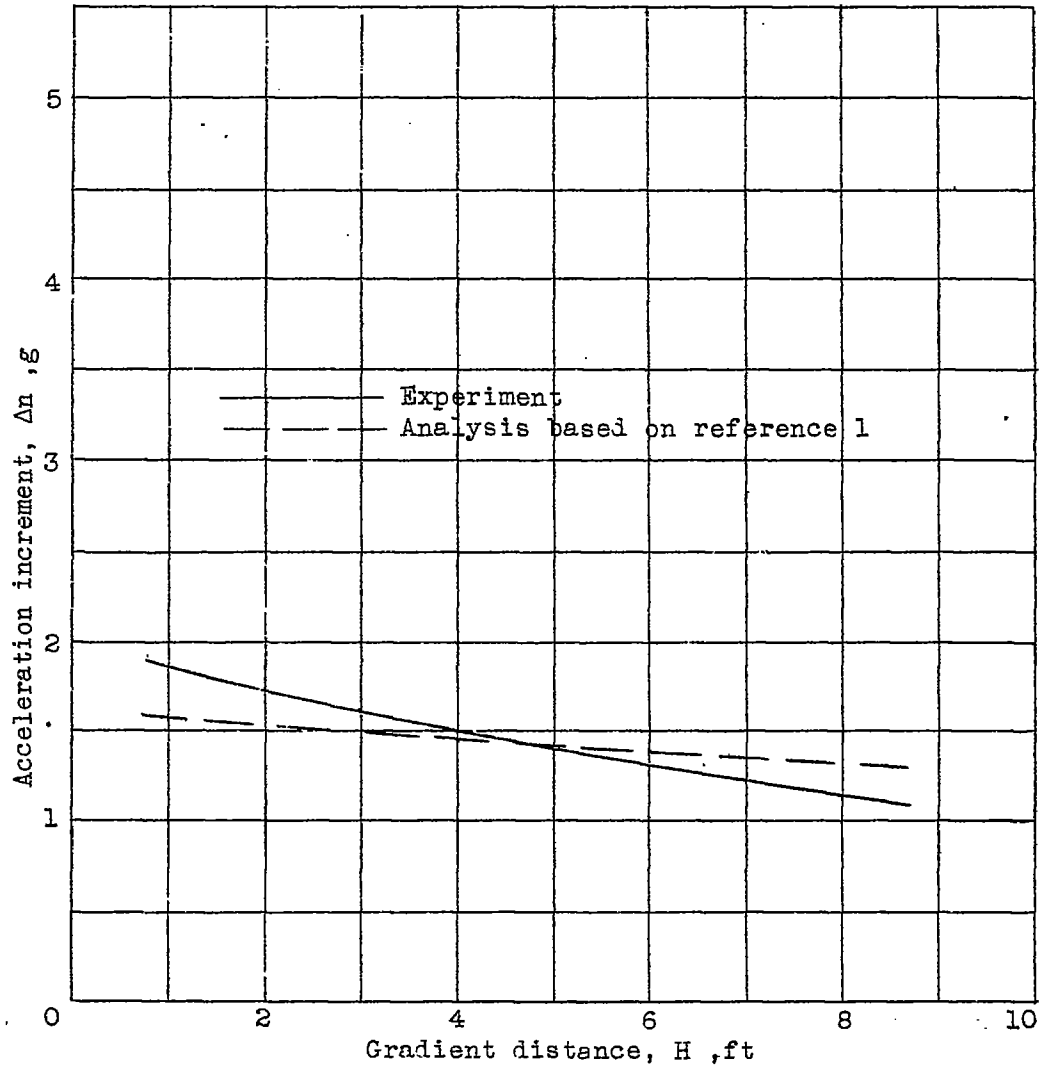

Figure 11.- Comparison of experiment and analysis, Boeing B-247